Razaz, Mahdi; Yano, Junki; Ishikawa, Kazuhiko; Kawanisi, Kiyosi

Application of Acoustic Tomography for Gaging Discharge of Atidally Dominated River

APPLICATION OF ACOUSTIC TOMOGRAPHY FOR GAGING DISCHARGE OF A TIDALLY DOMINATED RIVER

Mahdi Razaz[1], Junki Yano[2], Kazuhiko Ishikawa[3] and Kiyosi Kawanisi[4]

ABSTRACT

Fluvial acoustic tomography system (FATS) is an innovative technique for continuous monitoring of river velocity, particularly in tidal zones. The velocity can be computed from measuring the time it takes to perform reciprocal sound pulse transmission between at least two acoustic stations. This paper reports a field assessment of the quality of section-averaged velocities, directions and salinities derived from reports of two of couples of acoustic stations with crossing paths installed in upstream reaches of Ota Diversion Channel, Japan. Reference data were provided by a broadband Teledyne RD Instruments, Inc. (RDI) 1.2 MHz ADCP. Reference velocity and direction were established from moving average of three transects over discharge range of 0-25 m^3/s. The comparison with ADCP data revealed that there has been a consistent shift of 0.15 m/s in FATS velocity measurements. The reason why FATS velocities were biased persistently requires further investigations. For the mean flow direction, quantities deduced from the two instruments were not comparable. This inconsistency might be related to the larger zone covered by the FATS and that ADCP reports the direction using data across a line perpendicular to the river banks. Salinity measurements from a salinity sensor and those obtained from the instrument were in good agreement.

1. INTRODUCTION

Long-term knowledge of a river and its tributaries discharge is one of the most prominent factors in sustainable management, disaster prevention, control of water resources, and environment conservation in riverine and coastal zones. However, due to the complexity of flow in tidally dominated rivers quantifying river discharge and its direction is quite challenging. In recent years, several innovative velocity monitoring systems were applied to streamflow monitoring where the total discharge is computed from the cross-sectional bathymetry profile, the water height and velocity measurements in a more or less extended part of the cross section. Among these flow

[1] Researcher, Dept. of Civil and Environmental Engineering, Graduate School of Engineering, Hiroshima University, 1-4-1 Kagamiyama, Higashi-Hiroshima 739-8527, Japan (mrazaz@hiroshima-u.ac.jp)
[2] Graduate Student, Dept. of Civil and Environmental Engineering, Graduate School of Engineering, Hiroshima University, 1-4-1 Kagamiyama, Higashi-Hiroshima 739-8527, Japan (m120997@hiroshima-u.ac.jp)
[3] Graduate Student, Dept. of Civil and Environmental Engineering, Graduate School of Engineering, Hiroshima University, 1-4-1 Kagamiyama, Higashi-Hiroshima 739-8527, Japan (m123344@hiroshima-u.ac.jp)
[4] Associate Prof., Dept. of Civil and Environmental Engineering, Graduate School of Engineering, Hiroshima University , 1-4-1 Kagamiyama, Higashi-Hiroshima 739-8527, Japan (kiyosi@hiroshima-u.ac.jp)

monitoring techniques, sidelooking Doppler current profilers (H-ADCP) follow the same principle of operation as acoustic Doppler current profilers (ADCP) used to gauge rivers; they measure the horizontal water velocity profile along a limited horizontal line across the section (Le Coz *et al.*, 2008). But the Doppler method lacks the penetration capabilities of tomography equipment because it has greater susceptibility to interference from boundary conditions, and is subject to signal attenuation from the same particles necessary in backscattering the signal. Moreover, arrangement of large number of such sensors inside the target area is expensive and hard to maintain in long runs, and may be susceptible to damage by, for example, fishing activities or ferry boats. Acoustic Velocity Meters (AVM's) assume a straight line propagation to measure a representative index velocity (Simpson and Bland, 2000). As such, calibration error is usually found to be a substantial source of error in discharge estimation. Moreover, straight-line propagation assumption makes AVM's susceptible to the multipath phenomenon which occurs in its extreme forms in shallow waters, and also to the horizontal/vertical ray bending phenomenon caused by temperature or salinity gradients. Emerging noncontact techniques such as large-scale particle image velocimetry (LSPIV) allow the measurement of the surface flow velocities (Muste *et al.*, 2008). In this method measurements along vertical axis might not only be missed, they might also introduce interference in the data for the x/y–components caused by parallax particularly in non–unidirectional flows such as estuaries with complex vertical distribution of current velocity.

Fluvial Acoustic Tomography System (FATS) is based on travel-time tomography approach: measurements of travel-time values between a sound source and a receiver. In its basic form FATS consists of two broadband transducers with omnidirectional horizontal and hemispherical vertical beam patterns. Transmitting elements are triggered by an accurate GPS clock and simultaneously (or sequentially) emit modulated pulse with an adjustable frequency in the range of 10-30 kHz. Reciprocal sound transmission between each couple of monostatic transducers enables us to separate the influence of scalar factors, temperature or salinity, and flow on the effective sound speed. In contrast to other transit time flowmeters such as AVM's, sound rays propagated from transducers traverse the whole cross-section and therefore section-average velocity is directly quantified. In general, for each transmitted pulse there is a set of received pulses, characterized with different shapes, amplitudes, and delays. To accurately identify the arrival time of traveling sound mixed with noise, the transmitted signal is phase-modulated by applying the pseudo-random sequence (Simon *et al.*, 1985). Signal modulation scheme varies from one transducer to another that makes it also feasible to distinguish between received pulses with same arrival times but from different sources. FATS in its most basic form, including only a couple of transducers, has already been proven to be a prospective method for continuous monitoring of tidal river discharge and temperature/salinity variations (Kawanisi *et al.*, 2010). In this study, two couples of transducers with crossing paths were deployed in a site with large horizontal and vertical recirculation eddies to investigate the effect of strong horizontal/vertical salinity/temperature gradients on velocity measurements. Extra information from the second path is used for correcting errors in angularity that stem from intermittent flow direction changes. The main goal of this experimental study is to benchmark FATS results, section-averaged velocity and salinity, with those acquired from an ADCP and a conductivity sensor.

2. FUNDAMENTALS OF THE METHOD/THEORETICAL APPROACH

Acoustic travel-time tomography is based on a set of travel time measurements of acoustic signals between sound sources and receivers whose positions are known. The time that an acoustic wave requires to propagate from the source to the receiver is representative of the average sound speed

along the considered path. Scalar influences such as temperature or salinity affect the speed of sound independently of the direction of sound propagation, while the influence of flow depends on the direction. Various equations have been proposed to predict the acoustic velocity in water, among all Medwin (1975) proposed a formula for the sound speed c as a function of the temperature T ($^\circ$C), salinity S, and depth D (m) at $0 \le T \le 35^\circ$C , and $0 \le S \le 45$ m

$$c = 1449.2 + 4.6T - 0.55T^2 + 2.9\times10^{-4}T^3 + (1.34 - 0.01T)(S-35) + 0.016D \quad (1)$$

A flow component in the direction of sound propagation yields an increase of the effective sound speed, while it leads to a decrease in the opposite direction. Let us consider two acoustic stations, placed at horizontal spacing L in a fluid medium moving with velocity $\mathbf{v}$. The travel times t_1 and t_2 for the forward and reverse directions are calculated by the following formulae

$$t_1 = \frac{L}{c_m + u_m}; \quad t_2 = \frac{L}{c_m - u_m} \quad (2a,b)$$

respectively, where u_m is the mean along-ray velocity and c_m the mean sound speed along the transmission path. From eq. 2 the mean sound speed c_m and along-ray velocity u_m averaged along the sound path are respectively given by

$$c_m = \frac{L}{2}\left(\frac{1}{t_1} + \frac{1}{t_2}\right); \quad u_m = \frac{L}{2}\left(\frac{1}{t_1} - \frac{1}{t_2}\right) \quad (3)$$

In case of using two couples of acoustic stations with crossing paths i and j, the flow speed along each path is decomposed to components $\mathbf{v}_i = (u_i, v_i)$ and similarly $\mathbf{v}_j = (u_j, v_j)$ in a Cartesian coordinate system. Using basic vector operations $v_m = \sqrt{(u_i + u_j)^2 + (v_i + v_j)^2}$ and $\theta_F = \tan^{-1}\left[(u_i + u_j)/(v_i + v_j)\right]$, where v_m is the mean streamflow magnitude and θ_F is the azimuth angle of mean flow path on the horizontal plane.

3. FIELD SITE AND METHODOLOGY

3.1. Study Area

The Ōta River is a network of tidally–dominated rivers that flow through Hiroshima City, Japan. As seen in Figure 1(a) the main stream bifurcates into two main branches nearly 9 km before pouring into the Hiroshima Bay and the westernmost branch is called Ōta Diversion Channel. Arrays of sluice gates regulate amount of inflow to each branch. During normal days only 1/3 of the sluice gates are open providing a 30×0.3 m^2 cross section for diverting the flow into the channel. Field measurements were carried out during half of a complete cycle of a spring tide during 7 hours of April 8, 2012 in the upper reach of the Ōta Diversion Channel, Hiroshima, 275 m downstream from arrays of the sluice gates. In the measurement site under the influence of inflow from the sluice gates large horizontal eddies are formed and asymmetric tidal currents generate peak velocities as large as

0.5 m s^{-1} and 0.1 m s^{-1}, respectively, during the ebb and flood with a maximal tidal range of 1.5 m in a spring tide. Combination of asymmetric inflow and saline wedge intrusion generates strong halocline and transverse density gradients. In 2011, the river bed in the bifurcation zone upstream of the sluice gates was dredged and part of the loose bed materials were gradually washed away downstream. Larger sediments, mainly fine sand, settled and formed sandbars upstream of the observation site. Because of the river morphology near the observation site, the flow pattern varies with tidal phase (Figure 1b).

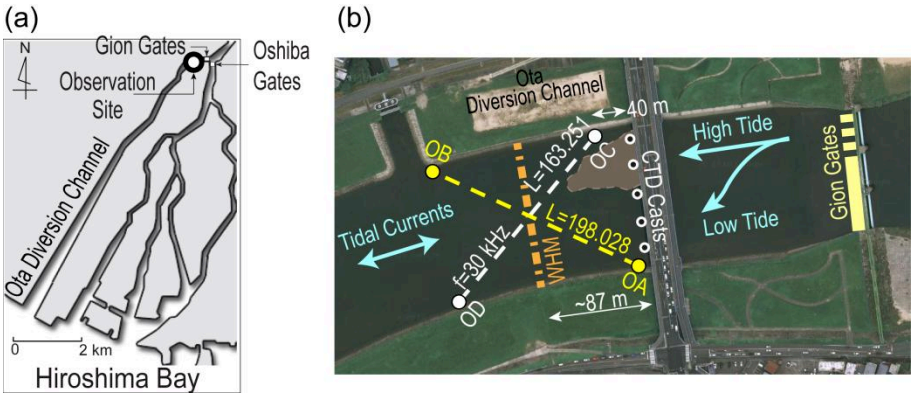

Figure 1 (a) Survey site marked in schema of Ota River network flowing through Hiroshima City, and (b) FATS setup as well as WHM track across the river. During low tide flow from Gion Sluice Gates is diverted towards southern half of the channel by sandbar.

A schematic of transducer location and WHM transect is displayed in Figure 2(b). Transducers with the approximate bandwidth of 20 kHz and source level of 197 decibels were employed in this study. For both pairs the frequency of the transmitted pulse was set to 30 kHz and the sampling frequency to 60 s. From our experience, installing transducers over loosely settled sandbars leads to weak bottom reflection and dampening of the transmitted pulse, therefore transducer OC was not installed exactly in the opposite shore relative to OA to avoid weak signal transmission. Note that in tidal zones with highly variable water level we should make a compromise between the maximal distance between each two transducers and duration they remain submerged. Thus a neap tide was selected for the test to allow installation of the transducers as close as possible to the banks. Distances between each couple of transducers were measured using a total station with $\pm(3+2\text{ppm}.L)$ mm accuracy.

To establish a set of reference discharge data for evaluating FATS nominally every hour a round-trip was made by a broadband RDI's 1200 kHz Workhorse Monitor ADCP (WHM) mounted on a boat. Water velocities were acquired through the pulse-coherent mode (mode 11). The velocity bin size was set to 0.02 m and measured velocities were 7-ping-averaged. All data were referenced to the ADCP bottom tracking. Drift in the bottom tracking due to moving bed effects or compass error were not significant.

Each transect began from or ended at the embankments. During each transect, the boat speed was maintained at approximately 0.25 m/s and as a result the travel time was less than 10 minutes. Transect width varied between 112 to 120 m depending on tide and maximal corresponding river depth variations were less than 7 cm within each 10 min. The ADCP discharges were directly extracted from WinRiver II software (Teledyne RD Instruments). The unmeasured near-shore discharge was negligible; however the missing discharge between the surface and the first ADCP cell was estimated by extrapolating the value of the first three good bins to the surface. This method

extrapolates data in a straight line to the surface. For the missing layer caused by side-lobe effect the bins present in the lower 20% of the depth were used to determine a power fit. The fit is forced to pass through zero at the bed. In the absence of any good bins in the lower 20% the last single good bin was used.

Salinity and temperature variations induced by tidal currents were observed by casting a JFE Advantech Compact-CTD (conductivity-temperature-depth sensor) at 5 points from a nearby bridge. The CTD depth resolution was set to 10 cm. Throughout the observation water surface was calm and only negligible wind–driven waves were detected by visual inspections.

4. RESULTS AND DISCUSSION

4.1. WHM and CTD Campaigns

In order to establish reference velocity data for evaluation of the FATS performance, 24 WHM river discharge measurements were performed during the observation window. The investigated discharge conditions ranged from nearly zero to 25 m^3/s. The hydraulic conditions were dramatically unsteady during the corresponding time span. Shown in Figure 2 is the along-channel velocity derived from WHM. Direction of the flow corrected using mean flow direction θ_R estimated from $\theta_R = \mathrm{Tan}^{-1}\left(\sum_{a}^{a=N} \sum_{b}^{b=n} v_{N_{ab}} \Big/ \sum_{a}^{a=N} \sum_{b}^{b=n} v_{E_{ab}} \right)$ where v_N and v_E are horizontal velocity components measured by WHM in ENU coordinate system, N is number of ensembles for each transect, and n is the number of valid bins in each ensemble. Positive velocity values denote currents towards downstream and negatives towards upstream. During the first half of flooding tide there is upstream directed flow only in the far southern part of the channel. However, in the second half of flood, a large recirculation eddy forms within the channel, with upstream directed flow in the northern half of the channel. As a result the net flow gradually diminishes and tends towards zero in high water slack. With ebb tide initiation two layer flow regime forms in the river: a thick layer of fresh water slides over the saline water mainly in the northern half of the channel, in the meantime in the southern half flow is more or less stagnant. At the second half of ebb tide sandbar blocks the freshwater inflow from the sluice gates and therefore strong flow with downstream direction shifts from the northern to the southern half of the channel.

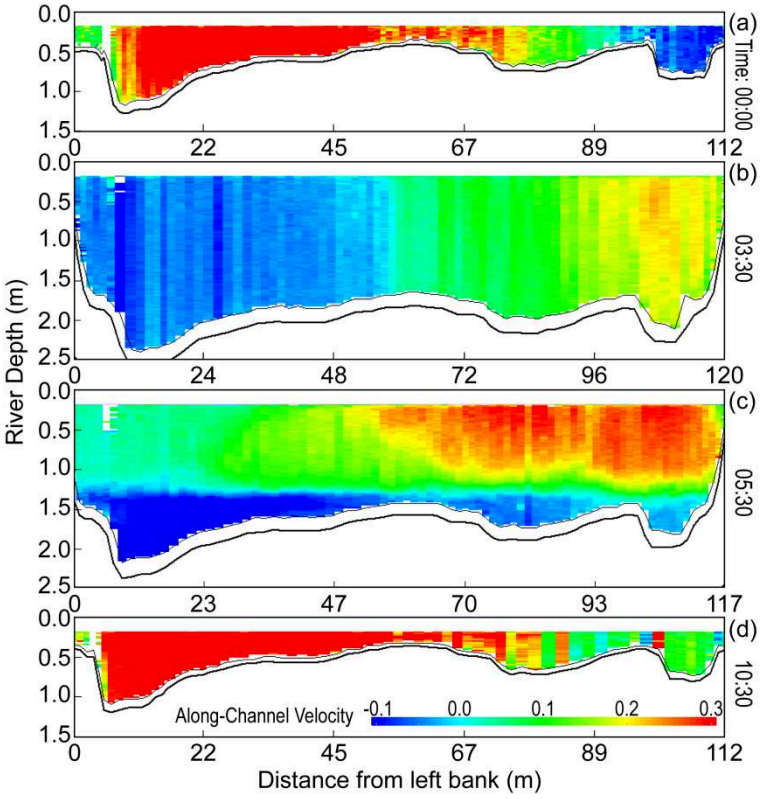

Figure 2 Typical flow regimes during the observation. Effect of the sandbar in diverting the freshwater flow in low tide is displayed in panels (a) and (d). (b) Large recirculation eddy forms within high water slack. (c) Two-layer flow forms during early stages of ebb. White areas in each panel denote the WHM transducer depth and unreliable velocity measurements caused by sharp variations in bed shape.

Figure 3 demonstrates the vertical salinity profiles selected at times corresponding to those shown in Figure 2 for two stations: St. 2 located 35 m and St. 4 that was 85 m far from the right bank.

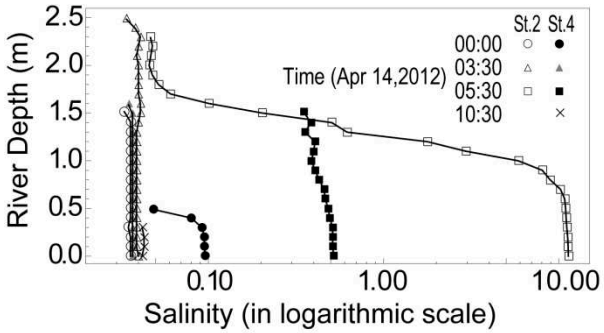

Figure 3 Typical vertical salinity profiles in logarithmic scale for St. 2 and St. 4 that were respectively 35 m and 85 m far from the right bank. St. 2 during low water slack was dried out.

4.2. Comparing FATS Measurements of mean Velocity with WHM

Using FATS with crossing paths variations of current speed mainly induced by tidal currents were observed for about 12 hours. Figure 4 illustrates instantaneous along-ray flow velocity variations driven by tidal currents resolved along OA-OB and OC-OD stations. Positive values indicate flow directions towards downstream and negative values stand for currents towards upstream. Due to vicinity of the observation site to sluice gates even during the flood general flow direction remains towards downstream. Having the geometry of transducers location and along-ray velocity components makes it possible to evaluate flow direction and magnitude. Figure 5 compares the results of the FATS with WHM. In this figure WHM data presented here are the moving averaged of each three consecutive data points. Using the simple vector calculation described in Section 2 magnitude and direction of section-averaged velocity can be deduced from the FATS along-ray velocity components and then the data are smoothed using a low-pass filter to see the average flow speed over a 30-min window. The cutoff period is selected considering the time it takes for the boat to make a two-way crossing of the river. As seen, there is a 0.15 m/s shift between velocity datasets reported by the two instruments. Because the velocity shift is consistent throughout the observation, the possibility of horizontal/vertical ray bending caused by saline wedge intrusion or transverse density gradient is cancelled. Moreover, ray tracing analyses (not shown here) for different flow conditions do not support dispersion or lack of penetration due to such phenomena. According to these analyses some rays however fail to penetrate to lower layers due to strong vertical density gradients, overlying rays with different launch angles indicate that at each pulse transmission there is a high probability that sound rays traverse the whole cross-section confined between each couple of transducers. Another possible source of error might be irregular variation in the flow angle. Fractional change in the velocity due to a change $\delta\theta$ in the flow angle is given by $\delta V/V = \tan\theta\,\delta\theta$ where $\delta\theta$ is expressed in radians. Shown in Figure 6 is the error caused by intermittent flow direction variation. Assuming that flow direction estimated from the crossing paths is correct, the error by caused by flow direction variation for OA-OB path remains less than 7%, though this error might be the dominant source of error along OC-OD path.

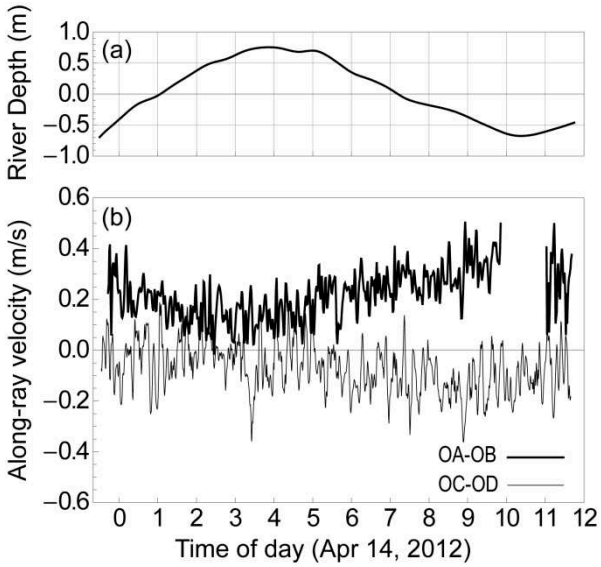

Figure 4 (a) River depth variation with tide. Zero is the sea level in Tokyo Bay. (b) Along-ray FATS velocity measurement at 1/60 Hz sampling frequency. During low water slack OB station dried out.

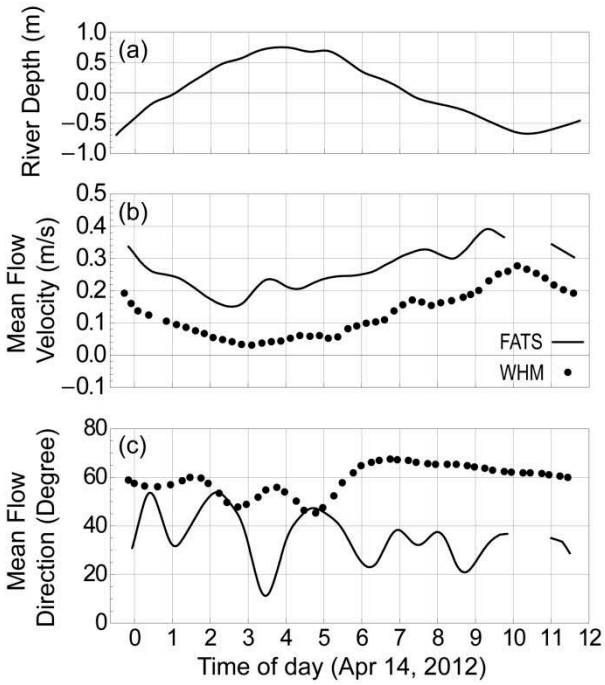

Figure 5 (a) River depth, (b) section-averaged velocity magnitude derived from FATS and WHM, and (c) section-averaged velocity direction. FATS data are low-pass filtered with a 30 min cutoff period.

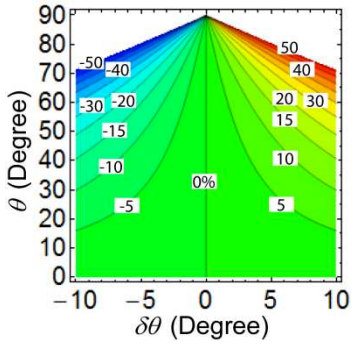

Figure 6 Relative error of flow velocity due to stream direction error

On the other hand, 20-40% of the WHM discharge is derived from extrapolation of the vertical velocity profile near the surface. As such, extrapolation error is potentially a substantial source of error in discharge estimation. Inspection of the WHM vertical velocity profiles indicates remarkable velocity gradient in the upper 0.25 layer which leads to trivial flow speed near the transducer. This issue might stem from near-field effects or we may assume a thin layer of fresh water sliding over the saline water. Compact CTD measurements however do not support the last hypothesis. Because there is no other reference data to compare the velocities of WHM and FATS with, it is hard to determine which sensor is functioning appropriately.

4.3. Comparing FATS measurements of mean salinity with Compact-CTD

In extremely shallow waters such as the observed site effect of depth in equation (1) can be neglected, therefore if the mean temperature is measured it would be possible to approximate the mean salinity. Figure 7 compares the cross-sectional mean salinity derived from CTD casts and those indirectly measured by the FAT.

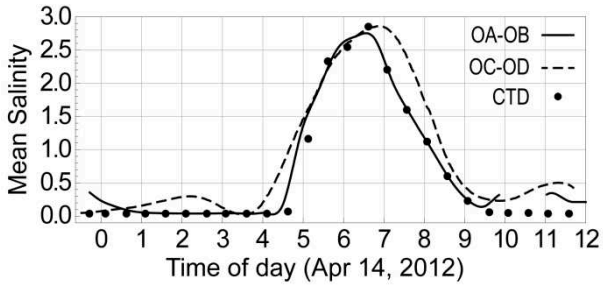

Figure 7 Section-averaged salinity measured by FATS and Compact-CTD. FATS data are averaged by a low-pass filter with 30 min cutoff period.

Salinity data from OA-OB path is in good agreement with the true mean salinity, path OC-OD however overestimate the salinity particularly after salinity peak (second half of the ebb). Salinity variation follows that of mean sound speed. Considering that path length assumed to be constant during the observation the overestimation of salinity might be related to underestimation of arrival time. Moreover, considering the complex velocity distribution, measuring only five points in the upstream boundary of the survey sight might not be a perfect representative for the area under study.

5. CONCLUSIONS

Section-averaged velocity measured by the FATS in upstream reaches of Ota Diversion Channel, Japan, were compared to concurrent ADCP measurements for 24 discharge values distributed over 0-25 m^3/s. FATS velocities were computed by transit time method. Once properly postprocessed, the FATS data were compared to WHM data deduced from velocity-area gauging. The comparison with WHM revealed that FATS velocity measurements were overestimated and there was a constant shift (0.15 m/s) from the true velocity. Further investigations are required to confirm which instruments reports the true velocity. Further comparisons between the salinity values computed from influence of scalar parameters (salinity and temperature) on underwater sound speed and those acquired directly from a CTD sensor indicated an acceptable consistency between the two sensors. However, salinity data from one of the paths were biased up under ebbing tide conditions. A physical robust method is required for salinity measurements inside the target area, while a limited number of direct salinity measurements over a small range are available.

REFERENCES

Kawanisi, K., Razaz, M., Kaneko, A., Watanabe, S. (2010). Long-term measurement of stream flow and salinity in a tidal river by the use of the fluvial acoustic tomography system. J Hydrol, 380, 74-81.

Le Coz, J., Pierrefeu, G., Paquier, A. (2008). Evaluation of river discharges monitored by a fixed side-looking Doppler profiler. Water Resour Res, 44.

Medwin, H. (1975). Speed of Sound in Water - Simple Equation for Realistic Parameters. J Acoust Soc Am, 58, 1318-1319.

Muste, M., Fujita, I., Hauet, A. (2008). Large-scale particle image velocimetry for measurements in riverine environments. Water Resour Res, 44.

Simon, M.K., Omura, J.K., Levitt, B.K. (1985). Spread Spectrum Communications Handbook, McGraw-Hill, New York.

Simpson, M.R., Bland, R. (2000). Methods for accurate estimation of net discharge in a tidal channel. Ieee J Oceanic Eng, 25, 437-445.